REPORT DOCUMENTATION PAGE

1. REPORT DATE *(DD-MM-YYYY)*	2. REPORT TYPE	3. DATES COVERED *(From - To)*
12-06-2007	Technical Paper	

4. TITLE AND SUBTITLE	5a. CONTRACT NUMBER
Experimental and Computational Observation of Radiometric Forces on a Plate (Preprint)	5b. GRANT NUMBER
	5c. PROGRAM ELEMENT NUMBER

6. AUTHOR(S)	5d. PROJECT NUMBER
N. Selden, C. Ngalande, S. Gimelshein (USC); A. Ketsdever (AFRL/PRSA)	5e. TASK NUMBER
	23080532
	5f. WORK UNIT NUMBER

7. PERFORMING ORGANIZATION NAME(S) AND ADDRESS(ES)	8. PERFORMING ORGANIZATION REPORT NUMBER
Air Force Research Laboratory (AFMC) AFRL/PRSA 10 E. Saturn Blvd. Edwards AFB CA 93524-7680	AFRL-PR-ED-TP-2007-322

9. SPONSORING / MONITORING AGENCY NAME(S) AND ADDRESS(ES)	10. SPONSOR/MONITOR'S ACRONYM(S)
Air Force Research Laboratory (AFMC) AFRL/PRS 5 Pollux Drive Edwards AFB CA 93524-7048	11. SPONSOR/MONITOR'S NUMBER(S) AFRL-PR-ED-TP-2007-322

12. DISTRIBUTION / AVAILABILITY STATEMENT

Approved for public release; distribution unlimited (PA #07228A).

13. SUPPLEMENTARY NOTES
For presentation at AIAA Conference, Miami, FL, 25-28 Jun 2007.

14. ABSTRACT

The radiometric force on several configurations of heated plates placed in a stagnant gas is examined experimentally on a high resolution thrust stand and numerically using the direct simulation Monte Carlo method. A wide range of pressures from 0.006Pa to 6Pa corresponding to Knudsen numbers from 20 to 0.02 is examined for nitrogen, argon, xenon, and helium test gases. It is shown that the force is maximum in the transition regime (Kn~0.1) and is heavily dependent on the plate area. It is also shown that the force is strongly correlated with the chamber size, decreasing with increasing chamber size.

15. SUBJECT TERMS

16. SECURITY CLASSIFICATION OF:			17. LIMITATION OF ABSTRACT	18. NUMBER OF PAGES	19a. NAME OF RESPONSIBLE PERSON
			SAR	13	Dr. Ingrid Wysong
a. REPORT	b. ABSTRACT	c. THIS PAGE			19b. TELEPHONE NUMBER *(include area code)*
Unclassified	**Unclassified**	**Unclassified**			N/A

Experimental and Computational Observation of Radiometric Forces on a Plate (Preprint)

N. Selden[1], C. Ngalande[1], and S. Gimelshein[2]
University of Southern California, Los Angeles, CA 90089

A. Ketsdever[3]
AFRL Edwards AFB, CA 93524

The radiometric force on several configurations of heated plates placed in a stagnant gas is examined experimentally on a high resolution thrust stand and numerically using the direct simulation Monte Carlo method. A wide range of pressures from 0.006Pa to 6Pa corresponding to Knudsen numbers from 20 to 0.02 is examined for nitrogen, argon, xenon, and helium test gases. It is shown that the force is maximum in the transition regime (Kn~0.1) and is heavily dependent on the plate area. It is also shown that the force is strongly correlated with the chamber size, decreasing with increasing chamber size.

I. Introduction

The repulsion and attraction of bodies induced by radiation received a great deal of attention from a number of prominent scientists in the 19th and 20th centuries[1]. The first published experiment was conducted by Abraham Bennet[2] who reported in 1792 the negative result of light shined on a paper vane suspended by a fiber thread in vacuum. At that time, he was unable to see any motion distinguishable from the effect of heat. The first successful experiment was conducted by Fresnel[3] who observed in 1825 a repulsion between two suspended foil vanes when sunlight was focused on them in a low-pressure container.

In the 1870s, William Crookes proposed different types of apparatus to investigate the radiometer effect[4,5]; one of them became known as the Crookes radiometer. It consists of an airtight glass bulb containing a partial vacuum with a set of vanes mounted inside the bulb on a spindle; the vanes rotate when exposed to light or another heat source. Crookes incorrectly suggested that the force causing the vanes to move was due to photon pressure. This theory was originally supported by J.C. Maxwell who had predicted this force. O. Reynolds had initially proposed a reasoning based on surface outgassing, and then presented a more rigorous explanation based on kinetic theory[6]. According to the latter theory, the gas in the partially evacuated bulb is the main driving force responsible for the rotation of the vanes.

Reynolds also took part in the experiments conducted by Schuster[7] that turned up the first experimental evidence of gas forces being the dominant cause of the radiometric effect. In this experiment, the radiometer case was suspended by parallel fibers and light was directed onto the vanes. The radiometer case was pushed in the direction opposite the vanes, proving that the radiometric phenomenon is caused by the interaction between the heated side of the vane and the gas. The kinetic theory explanation given by Reynolds is in fact a free molecule approximation of the radiometric effect: the molecules leaving the hot side leave with an increased velocity relative to those leaving the cold side. This leads to a larger momentum change on the hot side, and results in the motion of the vanes with the hot side trailing.

The situation is, however, different in transitional or near-continuum flow. The molecules with higher velocities leave the hot side of the vane and collide with incoming molecules. These collisions cut the surface flux more efficiently than those reflected on the cold surface. Essentially, this means that these effects compensate each other, and pressures in the center of the vane are equal. This theory was first proposed by Reynolds[8]. At about the same time, Maxwell[9] also showed that an unbalanced force exists near the edge of the heated side of the vane, where the heat flow in the gas is non-uniform. Almost fifty years later, Einstein presented a simple theory[10] that related the

---

[1] Graduate Student, Dept. of Aerospace and Mechanical Engineering, Student Member AIAA
[2] Research Assistant Professor, Dept. of Aerospace and Mechanical Engineering
[3] Group Leader, Propulsion Directorate, Edwards AFB, Senior Member AIAA.

force on the vanes to their perimeter. This edge dependence of the vane force has found partial confirmation in experimental work[11], where the force was found to depend on perimeter, although not to the extent Einstein has predicted. Since about that time, the edge theory has become widely accepted.

The inversely proportional dependence of the radiometric force of a vane placed in a temperature gradient, deriven by Einstein, is similar to the high-pressure part of the general dependence proposed by Bruche and Littwin[12] that combines both high and low pressure regimes as $F = 1/\{(a/p) + (p/b)\}$.

This expression reflects the fact that the radiometric force has a maximum at some pressure that depends on gas and geometric properties, quantitatively shown as early as 1919[13]. At low pressures, a free-molecular area force is the dominant one, with the force increasing with pressure. At high pressures, the collisional edge force becomes dominant, and the force decreases as pressure increases.

The strong interest in the radiometer problem since 1873 declined steadily after 1928, mostly because the issue of force production was considered closed, and no direct application for radiometric forces had been identified at that time. The phenomenon that drives Crookes' radiometer has been summarized by Draper[14] who in effect described our present understanding of it. A temperature gradient exists on the surface if tangential stresses are to arise. These stresses are the result of thermal transpiration, with the gas moving over the surface from the cold to the hot side. Following this explanation, the principal force that contributes to the rotation of the vanes in the pressure regime where the radiometer is most effective, is the force created near the edges (a zone with the dimensions of a mean free path λ, according to Einstein).

Lack of an obvious application may explain the miniscule interest in the problem in the second half of the last century, when only a few research papers on the subject were published[15], with other publications being historic analyses and overviews. The situation started to change over the last decade, when the radiometric phenomenon was found to be useful in a number of different micro- and large-scale devices. The radiometric force has been shown by E.P. Muntz[16] to be applicable to modern microactuator, where the direct simulation Monte Carlo (DSMC) method was used to model forces on vanes mounted on an armature. This method, along with experimental measurements, has been employed by Ota et al[17] to study a concept of an opto-microengine that uses radiometric forces. Subsequently, a series of papers by Passian with co-workers have been published[18,19], where radiometric phenomena was studied experimentally and analytically, mostly with application to microcantilevers. The use of radiometric forces as an approach to study gas-surface translational energy accommodation has also been mentioned by Passian et al in a third paper[20]. A new concept of a high-altitude aircraft supported by microwave energy that uses radiometric effects has also been put forward by G. Benford[21].

The new studies of the old radiometric phenomena have been supported on the one hand by modern technologies that allow more accurate measurements, and on the other hand by state-of-the-art numerical methods that rely heavily on parallel computing. These two factors, along with the revived interest in the application of radiometric phenomena, have prompted the authors to revisit the contribution of the "collisionless" (area) versus the "collisional'" (edge) forces to the total radiometric force.

The main objective of this work is to examine experimentally radiometric forces created by rarefied gas flows on heated plates of different shapes, and to analyze numerically the change in the total force as a function of gas pressure and chamber volume. While experimental measurement of the radiometric force has benefits of correctly accounting for different factors, such as gas-surface accommodation, internal structure of molecules, and complex three-dimensional geometries, numerical modeling provide detailed information of gas flow properties and surface parameters.

II. Experimental Setup

To study the role of area and edge forces on the plate, three radiometer vane geometries were used. Each of them consisted of a Teflon insulator sandwiched between two aluminum plates. A resistive heater was located between one of the plates and the Teflon insulator, and the temperature of the hot side of the device was maintained by varying the power input to the heater. Each of the plates and insulator are 0.32cm thick, and when assembled yield a device thickness of 0.95cm. Figure 1 shows a CAD model of the device used for both experimental and computational comparisons. The first device was a rectangle 3.81 x 12.7cm, the second device was a rectangle with exactly double the area having dimensions of 7.62 x 12.7cm, and the third was a circle with a diameter of 11.13cm with an area equivalent to that of the large rectangle.
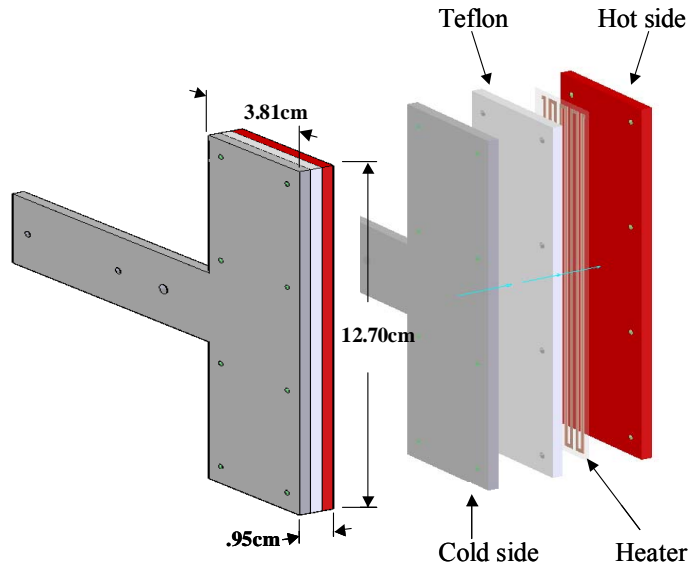
Figure 1. CAD drawing of a radiometric device

Each of these devices was individually mounted on a modified nano-Newton Thrust Stand (nNTS)[22] located inside of a 0.4m diameter vacuum chamber. When calibrated using a set of electrostatic combs[23], the nNTS provides very accurate and repeatable data with typical force resolution of approximately 0.1uN and statistical scatter around 1%. For the current experiment, the experimental error based on standard deviation ranges from a few percent at the lowest pressures to less than 1% through most of the curve. However, due to the normalization by experimental temperature measurements and the small uncertainty of the calibration method, the total absolute experimental uncertainty is ~4%. Day-to-day variation of multiple data sets has been observed to be ~1%.

The experimental data was obtained for each device by evacuating the chamber to a base pressure below 10^{-4} Pa. A constant voltage was applied to the heater, and this resulted in the main surfaces reaching temperatures of approximately 415K (hot) and 365K (cold). The background pressure inside the chamber was varied by flooding the chamber with a specific gas over a range of pressures from 0.1 Pa to 6 Pa. Argon, helium, and air were all utilized with the additional use of xenon.
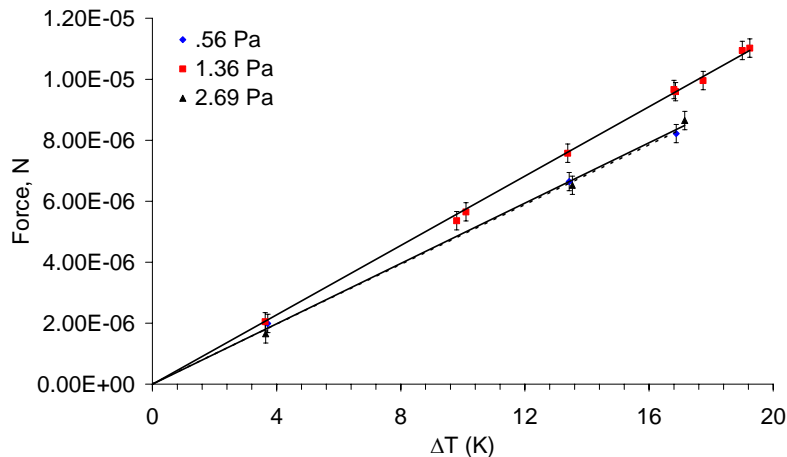

Figure 2. Changing force as a function of temperature difference across surfaces

The experimentally measured force was normalized by the temperature difference between the hot and cold plates, ΔT, for the purpose of comparing results for different pressures and gases. Verification of the validity of the experimental normalization method is demonstrated in Fig. 2, where exceptional linearity with temperature

3
American Institute of Aeronautics and Astronautics

Distribution A: Approved for public release; distribution unlimited

difference is observed. Three pressures are plotted at various temperature differences, where each pressure corresponds to a different flow regime. It is clearly shown that the force produced by the radiometer remains linear with ΔT regardless of which side of the maximum the data is taken.

III. Computational Setup

The direct simulation Monte Carlo computational tool, SMILE[24], was used in all DSMC computations presented in this work. The variable hard sphere model with parameters put forth by G.A. Bird [25] was used for the intermolecular potential, and the Larsen-Borgnakke model with variable rotational relaxation number used for translational-internal energy transfer. The gas-surface model was assumed to be diffuse with full energy and momentum accommodation. A two-dimensional module of SMILE was used in this work because three-dimensional modeling is prohibitively expensive for most pressures under consideration. The computations were conducted for two plates with dimensions 0.95x3.81cm and 0.95x7.62cm immersed in an initially uniform stagnant gas in a chamber. The third (Z axis) dimension of 12.7cm was assumed when calculating forces consistent with the actual size of the plate in the present experimental study. The main surfaces of the plate were set to 410K (cold) and 450K (hot), and the sidewalls were 430K. The chamber wall temperature was assumed to be constant at 300K. The computations were performed for chamber pressures ranging 0.006Pa to 6Pa and chamber sizes from 0.45cm to 1.8m using three gases: helium, nitrogen, and argon.

IV. Experimental and Computational Results

A. Vortex Structure

The flow field structure typical for the transitional regime around a plate is shown in Fig. 3, where the translational temperature and streamlines are shown for helium at a chamber pressure of 2Pa. The computation domain of 0.45x0.45m is bounded by 300K diffuse walls. The hot side is on the left hand side of the plate. There are four vortices created by the temperature gradients, two at each side of the plate. The vortices at the hot side of the plate are noticeably stronger than at the cold side. For the case under consideration, the maximum flow speed in the hot surface vortices is about 5m/s, and in the cold surface vortices it is about 2m/s.   Note that the vortex structure is similar to that calculated by Ota[17] but qualitatively differs from the flow structure given by Kennard[26]
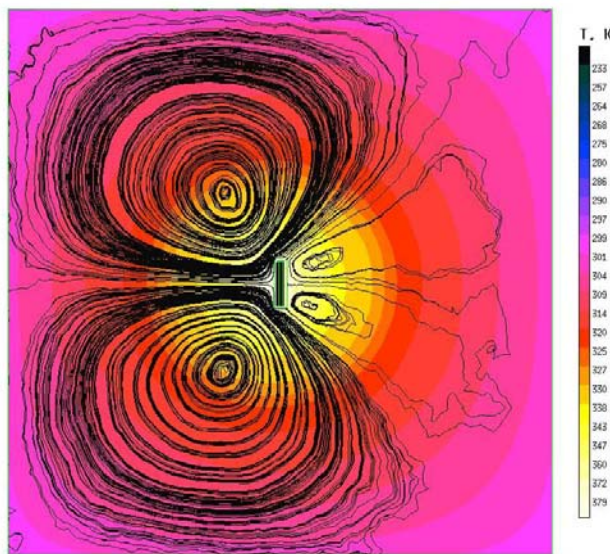

Figure 3. Flowfield around a radiometric device

B. The Effect of Gas Species

The forces from gas on hot and cold surfaces were computed, and the difference between the two (the net force) was analyzed for three carrier gases, helium, argon, and nitrogen. The net force for these gases as a function of pressure is given in Fig. 4.
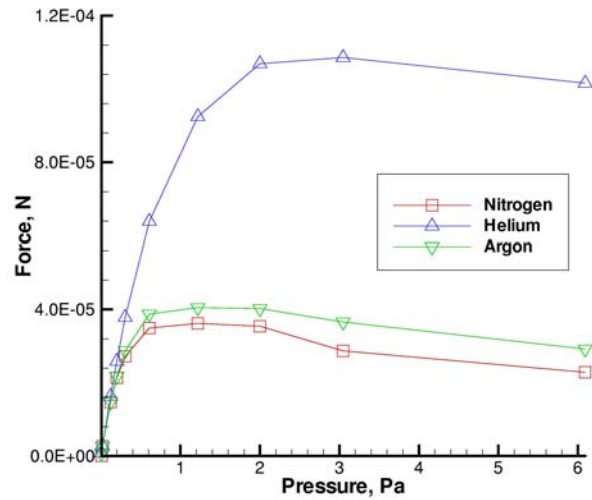
American Institute of Aeronautics and Astronautics

Figure 4. Computed force for various gases

It is seen that for every fixed pressure under consideration the force is maximum for the gas with maximum mean free path, helium; it is minimum for nitrogen, which has the smallest mean free path. This is related to the fact that the force per molecule is maximum in the free molecular regime, and it decreases as soon as molecules start colliding with each other, moreover, it tends to zero as the Knudsen number decreases.

The dependence of force on the mean free path of the gas is illustrated in Fig. 5, where the net force normalized by the force on the hot plate is shown as function of the Knudsen number calculated near the hot surface. There does not appear to be an impact of internal degrees of freedom for the temperatures under consideration. It is also important to note that the normalized force for three gases is within the error bars of the computational results that are estimated to be about 5% based on the statistical scatter of the surface properties.
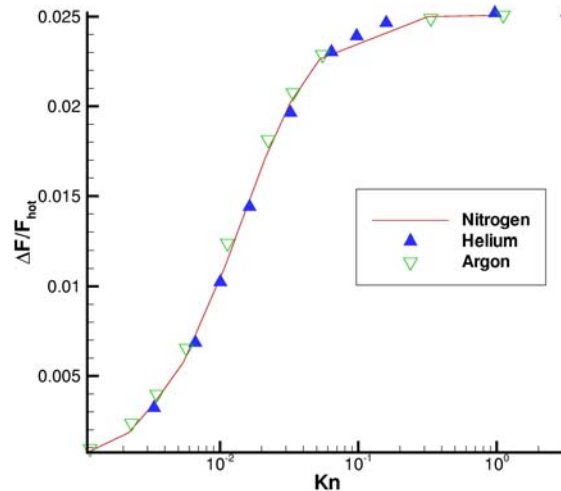

Figure 5. Normalized force *vs* Knudsen of various gases

Experimental results for the smallest device are shown in Fig. 6 and are normalized by the temperature difference across the plates. Normalization was necessary to account for differences in measured force due to slight changes in the magnitude of the gradient over the course of the experiment.
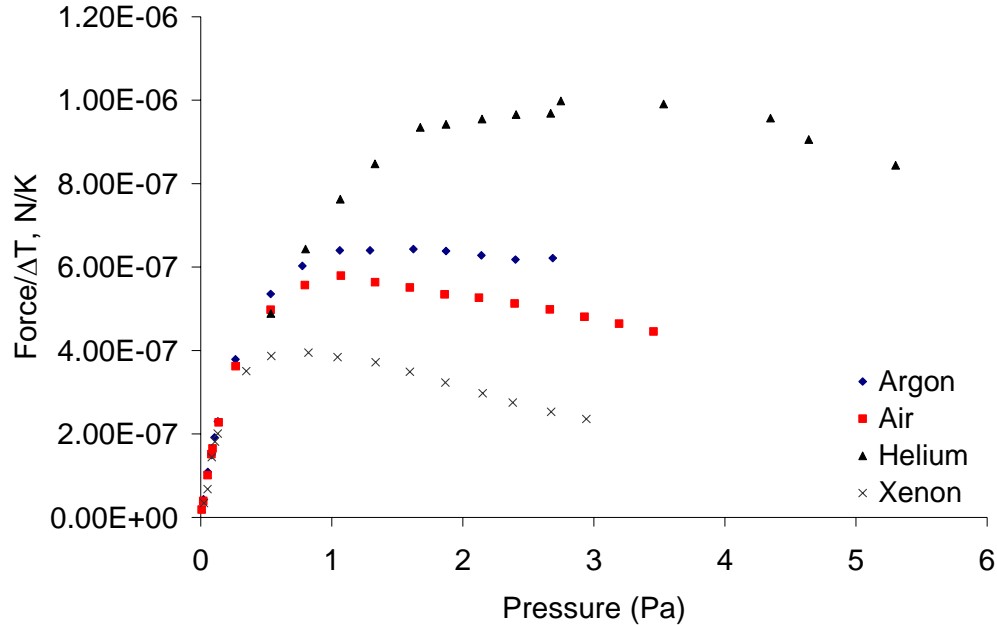

Figure 6. Experimental results for various gases

A qualitative comparison of the experimental and computational results displays similar behavior in trend and peak location. It is readily noted that helium produces a much smaller force proportionally in the experiment. The authors believe this is caused in part by the low energy accommodation of helium.

After comparing the low pressure results from these initial experiments with calculations in the collisionless regime, it was discovered that undesirable heat transfer to the nNTS was decreasing the experimentally measured force. This reduction was due to a temperature gradient opposite that of the experimental which acted as a 2nd radiometer. In all following experimental plots, this situation was remedied by taking the experimental data twice: once in the original configuration, and once in a reversed configuration. By taking the average of the two data sets the effect of the 2nd radiometer was removed.

C. Geometry Considerations

To examine the contribution of the edge effects to the net force, and analyze the relative importance of the forces on the edges of plate versus the area forces, the computations were performed in helium, for two geometric configurations, (i) a solid 3.9cm plate, and (ii) a 3.9cm plate that has ten 1mm holes. Consider first the surface pressure distribution over the cold and hot sides of the solid plate, shown in Fig. 7 for a chamber pressure of 2Pa.
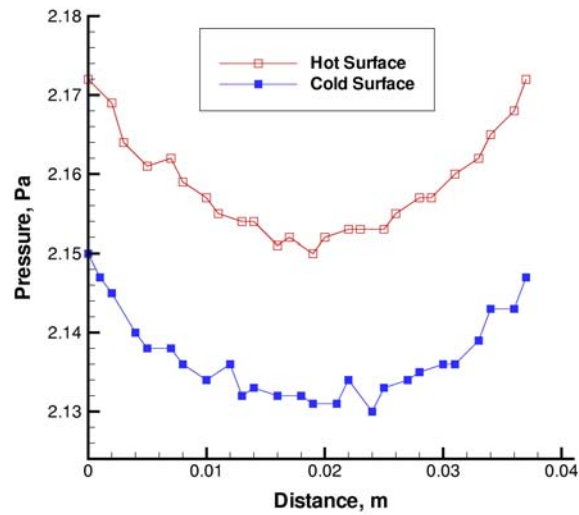
Figure 7. Pressure on main surfaces of the radiometer

The pressure has a minimum near the center of the plate both for the hot and cold sides. The values near the edges are visibly larger than that near the center. The net force, however, is produced by the difference of pressure forces on the hot and cold sides of the plate, and this difference is nearly constant for different distance stations along the plate. This is an indication that the area contribution is important to the net force. An additional confirmation to this statement is given in Table 1. The force on a hollow plate is generally lower than that on a solid plate, except for the 6Pa case where it is within the error bar of the computations.

Table 1. Comparison of solid and hollow plates

Pressure: 0.006 Pa		
	Solid Plate	Hollow plate
Hot surface	2.88430E-5	2.15860E-5
Cold Surface	-2.81203E-5	2.15860E-5
Net Force	7.22630E-7	5.49579E-7
Pressure: 2 Pa		
	Solid Plate	Hollow plate
Hot surface	1.01827E-2	6.85919E-3
Cold Surface	-1.00775E-2	-6.77046E-3
Net Force	1.05428E-4	8.85723E-5
Pressure: 6.092 Pa		
	Solid Plate	Hollow plate
Hot surface	3.00330E-1	2.04556E-2
Cold Surface	2.99301E-2	-2.03487E-2
Net Force	1.02870E-4	1.06145E-4

Experimental results for nitrogen in the small chamber are shown in Fig. 8. It is readily observed in the low pressure region that the circular plate and large rectangular plate collapse onto each other and that their values are very close to twice that of the smaller plate. This is expected, as free molecular theory shows the force to be entirely dependent on area. As the flow transitions from the collisionless regime, the picture becomes distinctly more clouded. While it is readily observed that the plates with larger area produce more force at their respective peaks, the force/area ratio does not hold.
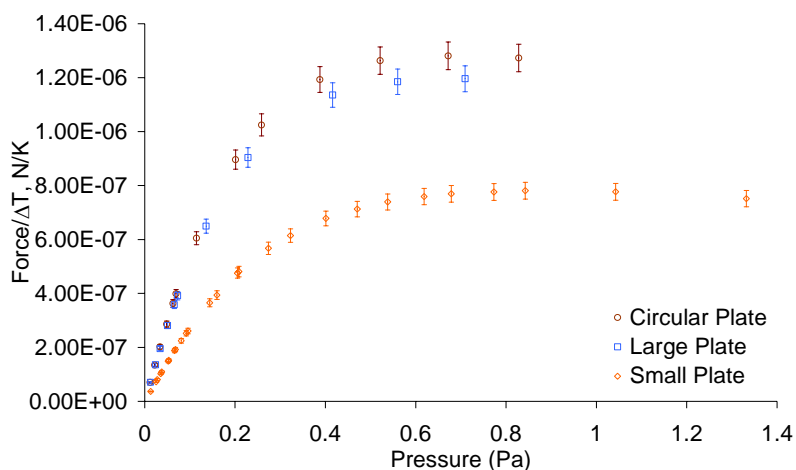
American Institute of Aeronautics and Astronautics

Distribution A: Approved for public release; distribution unlimited

Figure 8. Normalized force for different device geometries in the 0.4m chamber

When comparing the peaks of the large and small rectangles, it is found that the small plate creates 65% of the force of the larger one. Interestingly, this is almost precisely half way between the area ratio (50%) and the perimeter ratio (81%). Were that the only data presented, it would be tempting to presume that the perimeter force was slowly beginning to dominate. This does not entirely appear to be the case however, as the peak force created by the circle is decidedly larger by ~7%. It seems quite contradictory to accepted theory that a device with 14% less perimeter would create a larger force without an equivalent increase in heated surface. This increase in force is possibly explained by more efficient pressure redistribution in front of the plate due to the axial symmetry of the circular plate vortices.

The numerical predictions obtained for two different plate sizes are shown in Fig. 9 and are qualitatively similar to the above measurements. In the free molecular regime the larger plate produces a proportionally larger force. The ratio of the small plate force to the large plate force increases with pressure and reaches ~0.7 in the range of pressures where the force is maximum. This furthers the case that the area is still a large contributor to the peak force, where it must be noted that the perimeter ratio of the 2-D case is unity.
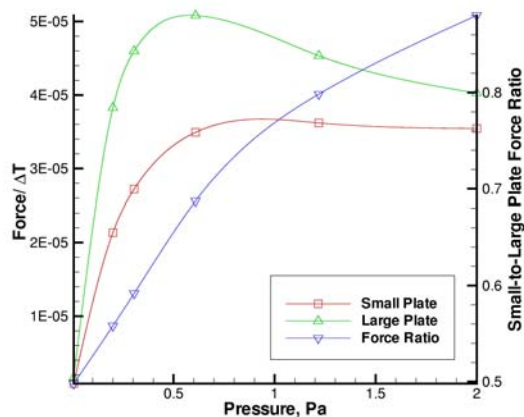

Figure 9. Numerical results for two different plates

Comparison of the DSMC results and experimental measurements of the net force on the plate in nitrogen is shown in Fig. 10 for different pressures. The force is normalized by the temperature difference between the cold and hot surfaces, since the actual values of the temperature somewhat varied in the experiment. The comparison shows that both measurements and DSMC predict pressure maximum around 1 Pa. The numerical results noticeably

overpredict the measurements, with the difference attributed primarily to the three dimensionality of the experiment and an incomplete energy accommodation that was not accounted for in DSMC.
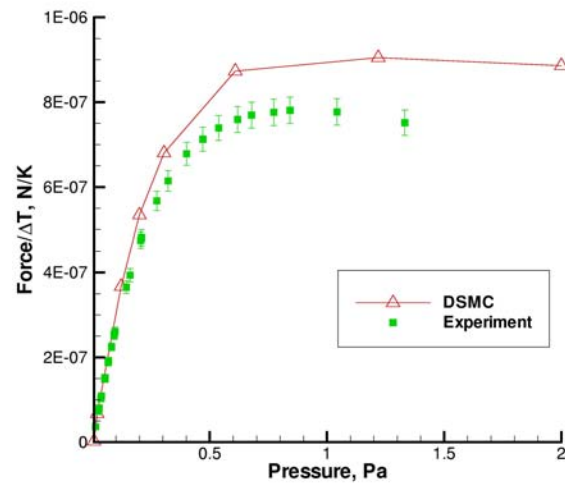

Figure 10. Comparison of experimental and computational results

D. Chamber Effects

The impact of the chamber walls has been studied for a helium flow at 2Pa with the chamber size varied from below 0.2m to about 1.8m with the boundary conditions on the plate and chamber walls unchanged. The analysis of the flow field shows that even when the chamber is about a hundred times larger than the heated plate, there is still pronounced effect of the location of the chamber walls on the flow properties not only near the chamber walls, but also near the plate. This is illustrated in Fig. 11 where the temperature profiles are shown for different chamber sizes in the cross section perpendicular to the plate and coming through its center. The plate center is at X=0.
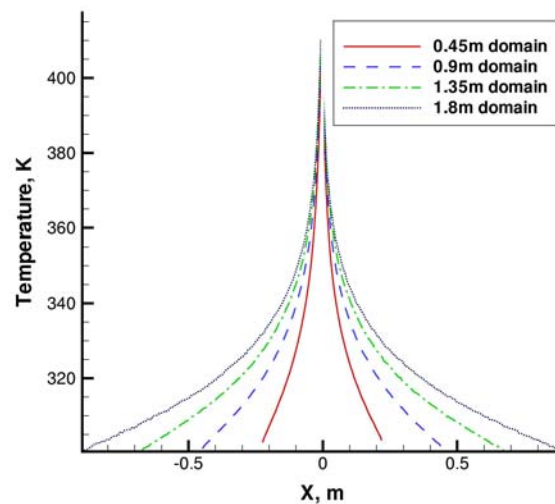

Figure 11. Temperature gradient in the gas as a function of chamber

Generally, the increase in the chamber size results in decrease of temperature and pressure gradients near the plate. As a result, the net force exerted on the plate decreases for larger chamber sizes, as shown in Fig. 12. It is also shown that a rapid increase in force occurs as the chamber size decreases, and it is expected to further increase until the free molecular limit is reached.
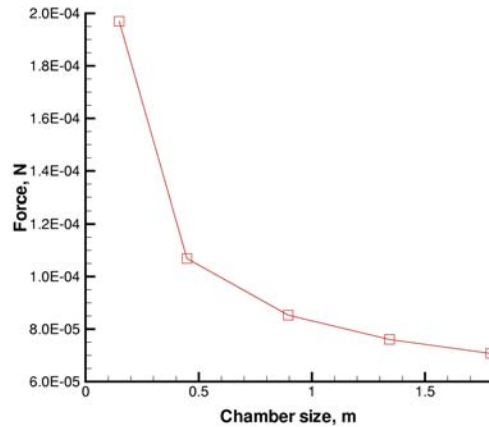

Figure 12. Force as a function of chamber size

After noticing that the computational values of the force diminished in increasingly larger chambers, the entire experimental setup was moved into a 3m diameter vacuum chamber (CHAFF). Experimental data for the larger chamber was taken in much the same way, but due to the facility change the upper boundary of the pressure measurement was drastically reduced from 6 Pa to ~1 Pa.

Results for nitrogen in the large chamber are presented in Fig. 13. While similar trends are observed when compared with the small chamber data, it is obvious that the chamber itself has a dramatic effect. For the large chamber, the peak of each device occurs at approximately ½ the pressure of the peak in the small chamber. There is also a noticeable decrease in the maximum force, as the largest measured data in the small chamber was 1.28×10^{-6} N/K while in the large it was 7.53×10^{-7} N/K.
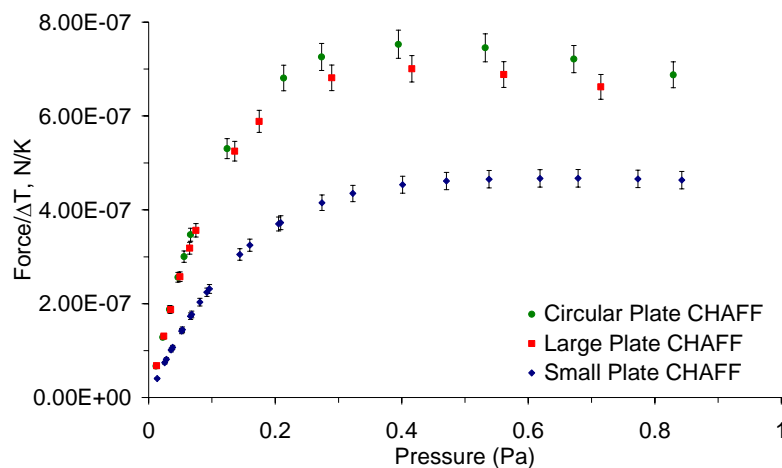

Figure 13. Comparison of device geometries in the 3.0m chamber (CHAFF)

The reduction in force due to increasing chamber size is better shown in Fig. 14 where chamber comparisons for each geometric configuration are shown. For each device the data behaves as predicted in the low pressure region, where it can be presumed that vortex and collisional contributions are minimal. As the pressure increases the force becomes noticeably stronger in the smaller chamber. This makes physical sense when compared with the limiting case of a chamber that is only slightly larger than the device; the device will behave as if it were

10
American Institute of Aeronautics and Astronautics

Distribution A: Approved for public release; distribution unlimited

collisionless so long as the mean free path of a gas molecule is longer than the distance between the device and the chamber wall.

a. Circular device

b. Large rectangular device

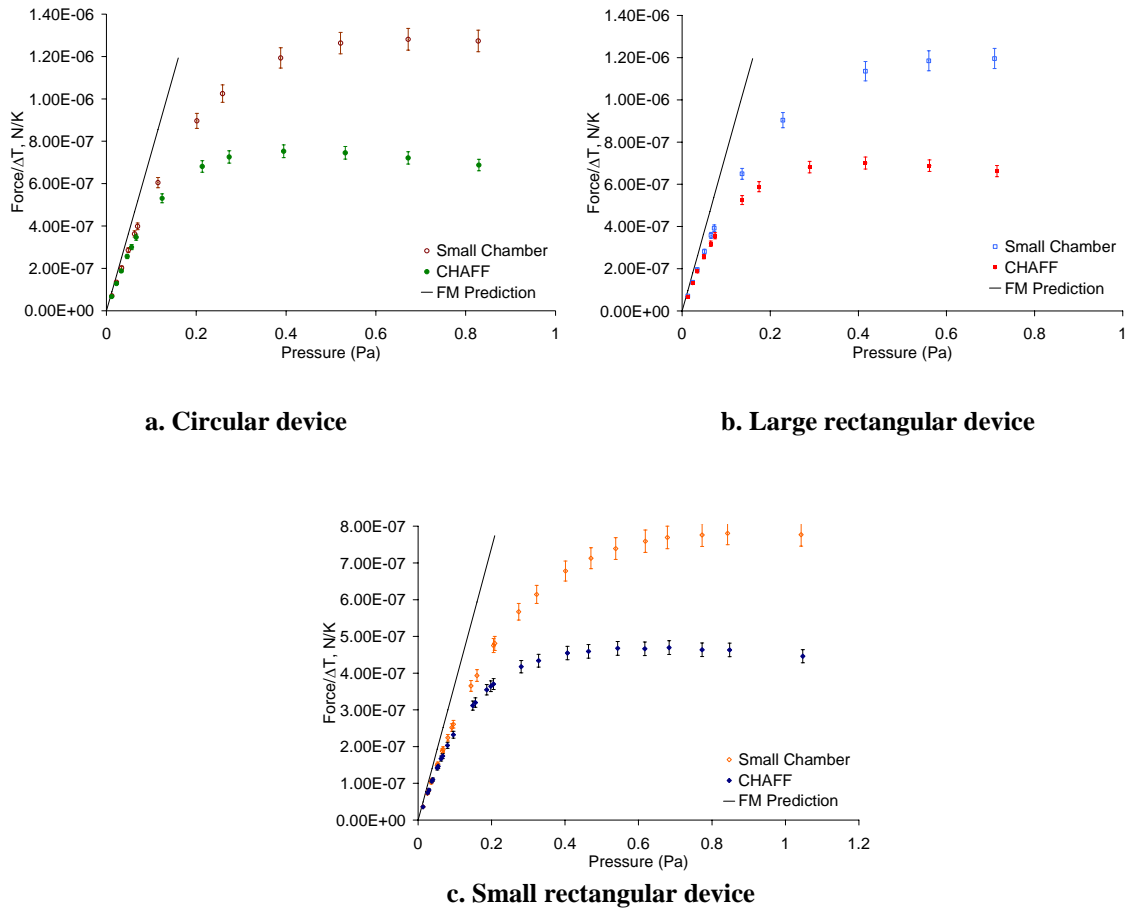**c. Small rectangular device**

Figure 14a, b, c. Comparison of device dependence on chamber size for three geometries

Further clarification is provided in Fig. 15, where the ratios of curves fit to the data sets for each device are compared. It is clearly shown that the larger plates behave very similarly. Not much can be concluded about the slight deviation between them in the middle of the pressure range as this falls within the bounds of experimental uncertainty. There is however a significant deviation from the small plate, presumably caused by the fact that the small plate is less affected by the shrinking chamber. This occurs because the larger plates are proportionally closer to the chamber wall, and thus are more likely to be affected by it.
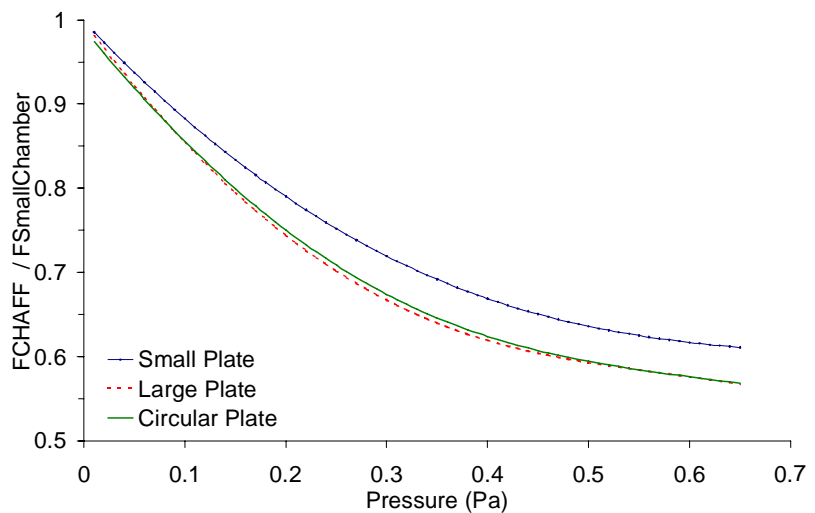

Figure 15. Ratio of curve fit data for a given device geometry

11
American Institute of Aeronautics and Astronautics

Distribution A: Approved for public release; distribution unlimited

V. Conclusion

A study of the radiometric forces on heated plates has been conducted both experimentally and computationally. The experiments were carried out at USC in two vacuum chambers up to a maximum pressure of 6 Pa for various carrier gases. The computations were performed with the DSMC method for a 2-D gas flow over a comparable range of pressures. It is shown that the radiometric devices provide maximum force at a Knudsen number approximating 0.1. Of the various gases tested, helium provides the largest peak force. Qualitatively, the experimental data and computational results are similar. A lack of experimental data on gas-surface accommodation and flow three-dimensionality yields approximately a 25% difference in the magnitude of the measured and computed forces. Comparison of three geometric configurations has shown that the effect of the area is significant at pressures up to where the force is maximum. It is also demonstrated that the size of the chamber in which the radiometer resides is of primary importance, where the size of the chamber is inversely related to the generated force.

References

[1] A.E. Woodruff, "William Crookes and the radiometer", Isis {57 (2)}, 188 (1966)

[2] A. Bennet, "A new suspension of the magnetic needle invented for the discovery of minute quantities of magnetic attraction", Phil. Trans. R. Soc. London, {82}, 81 (1792)

[3] A. Fresnel, Annales de Chimie et de Physique, {29}, 57 (1825)

[4] W. Crookes, "On attraction and repulsion resulting from radiation," Phil. Trans. R. Soc., {163} 277 (1873)

[5] W. Crookes, "On attraction and repulsion resulting from radiation," Phil. Trans. R. Soc., {165} 519 (1875)

[6] O. Reynolds, "On the forces caused by the communication of heat between a surface and a gas; and on a new photometer," Phil. Trans. R. Soc., {166} 725 (1876)

[7] A. Schuster, Phil. Trans. R. Soc., {166} 715 (1876)

[8] O. Reynolds, Phil. Trans. R. Soc., {170} 727 (1879)

[9] J.C. Maxwell, On stresses in rarefied gases arising from inequalities of temperature,"Phil. Trans. R. Soc., {170} 231 (1879)

[10] A. Einstein, "Zur theorie der fadiometerkrafte," Z. Physik, {27} 1 (1924)

[11] H. E. Marsh, J. Opt. Soc. Amer., {12}, 135 (1926)

[12] E. Bruche, W. Littwin, "Experimental contributions to the radiometer question," Z. Physik, {52,} 318 (1928)

[13] W. H. Westphal, "Messungen am Radiometer," Zeit. fur Physik, {1}, 92 (1920)

[14] C. W. Draper, "The Crookes radiometer revisited," J. Chem. Education, {53}(6), 357 (1976)

[15] E. A. Mason, B. Block, "Molecular inelastic collision cross sections from the radiometer force," Annals of Physics, {1}, 7 (1966)

[16] D.C. Wadsworth, E.P. Muntz, "A computational study of radiometric phenomena for powering microactuators with unlimited displacements and large available forces," J. Microelectromech. Syst., {5}(1), 59

[17] M. Ota, T. Nakao, M. Sakamoto, "Numerical simulation of molecular motion around laser microengine blades," Math. and Computers in Simulation, {55}, 223 (2001)

[18] A. Passian, A. Wig, F. Meriaudeau, T.L. Ferrell, T. Thundat, "Knudsen forces on microcantilevers," J. Appl. Phys., {92}(10), 6326 (2002)

[19] A. Passian, R. J. Warmack, A. Wig, et al., "Observation of Knudsen effects with microcantilevers," Ultramicroscopy, {97},401 (2003)

[20] A. Passian, R. J. Warmack, T.L. Ferrell, T. Thundat, "Thermal transpiration at the microscale: a Crookes cantilever," Phys. Rev. Letters, {90}(12) 124503 (2003)

[21] G. Benford, J. Benford, "An aero-spacecraft for the upper atomosphere supported by microwaves," Acta Austonautica, {56}, 529 (2005)

[22] A.J. Jamison, A.D. Ketsdever, and E.P. Muntz, "Gas dynamic calibration of a nano-Newton thrust stand," Review of Scientific Instruments, Vol. 73, 3629-3637, 2002.

[23] N.P. Selden, A.D. Ketsdever, "Comparison of force balance calibration techniques for the nano-Newton range," Review of Scientific Instruments, Vol. 74, 5249-5254.

[24] Ivanov, M.S., Markelov, G.N., Gimelshein, S.F. "Statistical simulation of reactive rarefied flows: numerical approach and applications," AIAA Paper 98-2669, June 1998.

[25] Bird, G.A., *Molecular Gas Dynamics and the Direct Simulation of Gas Flows*, Clarendon Press, Oxford, 1994.

[26] Kennard, E.H., "Kinetic Theory of Gases," McGraw-Hill Inc., New York, 1938